Superparamagnetic behavior in a Ni vermiculite intercalation compound

Masatsugu Suzuki* and Itsuko S. Suzuki
Department of Physics, State University of New York, Binghamton, New York 13902-6016

N. Wada
Department of Mechanical Engineering, Faculty of Engineering, Toyo University, 2100 Kujirai, Kawagoe City, Saitama 350-8585, Japan

M. Stanley Whittingham
Department of Chemistry, State University of New York, Binghamton, New York 13902-6016
(Received 11 August 2000; revised manuscript received 4 June 2001; published 22 August 2001)

The Ni vermiculite intercalation compound (VIC) magnetically behaves like a quasi two-dimensional (2D) Ising-like site-random ferromagnet on the triangular lattice sites, with weak antiferromagnetic interplanar interactions. The magnetic properties of Ni VIC have been studied using superconducting quantum interference device (SQUID) DC magnetization and SQUID AC magnetic susceptibility measurements. The 2D ferromagnetic short-range order of Ni^{2+} spins starts to grow below 45 K. A partially disordered antiferromagnetic phase is established below $T_N(=21.0\,\mathrm{K})$, where 2D ferromagnetic Ni clusters are antiferromagnetically coupled along the *c* axis. The dispersion χ'_{cc} along the *c* axis shows a peak around 2–3 K shifting to the low-temperature side with increasing AC frequency. Temperature dependence of the corresponding average relaxation time is well described by a generalized Arrhenius law. The system may be formed of disordered antiferromagnetic clusters, exhibiting a superparamagnetic behavior.

DOI: 10.1103/PhysRevB.64.104418 PACS number(s): 75.50.Lk, 75.40.Gb, 75.40.Cx, 75.70.Cn

I. INTRODUCTION

Vermiculite intercalation compounds (VIC's) with magnetic species inserted into their gallery space, are considered to provide a model system for studying two-dimensional (2D) magnetic systems.[1–5] The magnetic layers are separated by insulating host layers, which are about 9.5 Å thick. The separation distance between the adjacent magnetic layers is on the order of 14.4 Å. To date, however, they have not been systematically exploited in this perspective. VIC's are well-characterized expanding layered silicates, where each host silicate layer is composed of two tetrahedral sheets coupled symmetrically to an octahedral sheet. In order to balance the charge deficiency due to isomorphic substitution of Al^{3+} for Si^{4+} in tetrahedral sheets, the cations are introduced into the interlamellar space between the host silicate layers. Naturally occurring vermiculite has Mg^{2+} ions as cations and is denoted by Mg VIC. Mg^{2+} ions in the interlamellar space between the host silicate layers can be easily exchanged by various kinds of magnetic ions such as Mn^{2+}, Co^{2+}, Ni^{2+}, and Cu^{2+}, forming magnetic VIC's.[2] The magnetic VIC's have three kinds of hydration states (HS) defined by the number of water layers (WL) in the interlamellar space; zero-, one-, and two-water-layer hydration states.[6] In the one-WL HS the water molecules normally lie in the same plane as the cations. In the two-WL HS, the magnetic cations are usually sandwiched between upper and lower water layers. The hydration state depends on the water vapor pressure and temperature. The magnetic VIC's are frequently in the two-WL HS under normal ambient conditions.

There have been several studies on the magnetic properties of magnetic VIC's. Suzuki *et al.*[2] have measured the DC magnetic susceptibility of Mn, Co, Ni, and Cu VIC's with two-WL HS in the presence of magnetic fields ($H=4$ kOe, 11.8 kOe). They have claimed that these compounds show no magnetic phase transition in the temperature (T) range between 4.2 and 300 K. The DC magnetic susceptibility obeys the Curie-Weiss law. The Curie-Weiss temperature Θ of Ni VIC with two-WL HS is positive, indicating that the intraplanar exchange interaction is ferromagnetic. The Curie-Weiss temperature of Mn, Co, and Cu VIC's with two-WL HS is close to zero but negative. The unit-cell stoichiometry of magnetic VIC's with two-WL HS has been determined from DC magnetic susceptibility and thermogravimetric measurements.[2] The number of cations in the unit cell was determined as $u=0.76\pm0.08$ for Mn, Co, and Ni VIC's and $u=1.12\pm0.07$ for Cu VIC. Zhou *et al.*[4] have also reported the results of DC magnetic susceptibility for Mn, Co, Ni, and Cu VIC's having zero- and two-WL HS in the temperature range between 2 and 300 K. They have shown that (i) only Ni VIC with two-WL HS has a positive Curie-Weiss temperature ($=4.13$ K), and that (ii) Co and Ni VIC's with zero-WL HS undergo antiferromagnetic phase transitions at 5 K and 3 K respectively. Nishihara *et al.*[3] have measured the field (H) dependence of magnetization for Ni VIC with two-WL HS at 4.2 K in the presence of H along the *c* axis up to 270 kOe. They have shown that the high-field magnetization in Ni VIC with two-WL HS is well described by a model of quasi-2D magnetic system with predominant ferromagnetic intraplanar exchange interaction and weak antiferromagnetic interplanar exchange interaction. Wada *et al.*[1] have reported a preliminary result on AC magnetic susceptibility of Ni VIC with two-WL HS, indicating some evidence for magnetic phase transitions at 2.3 and 3.4 K.

In this paper we have undertaken an extensive study on the magnetic properties of Ni VIC with two-WL HS using superconducting quantum interference device (SQUID) DC magnetization and SQUID AC magnetic susceptibility. This

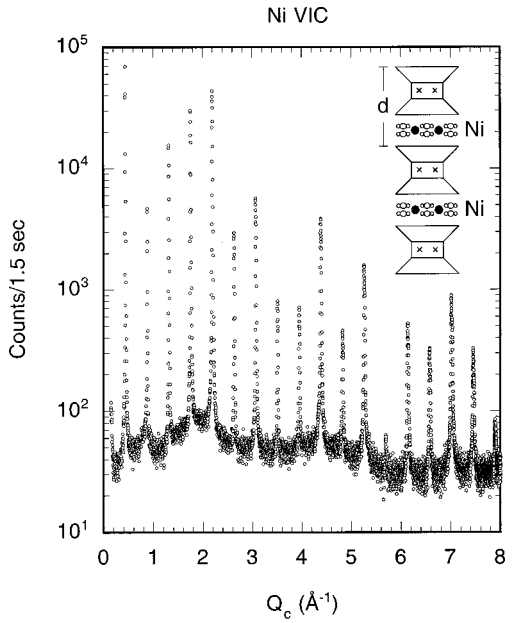

FIG. 1. (00L) x-ray diffraction pattern of Ni VIC with two-WL HS. The inset shows the schematic structure of Ni VIC composed of two tetrahedral sheets and one octahedral sheet. The locations of Ni^{2+} (●) and Fe (×) are shown in the inset. The *c*-axis repeat distance is $d=14.330\pm0.007$ Å.

compound magnetically behaves like a quasi-2D Ising-like site-random ferromagnet with a very weak antiferromagnetic interplanar exchange interaction. The spin easy axis is the *c* axis. This compound shows an antiferromagnetic phase transition at $T_N(=21.0\,\mathrm{K})$. The dispersion χ'_{cc} along the *c* axis shows a peak around 2–3 K, shifting to the low-temperature side with increasing an AC frequency *f*. The average relaxation time τ is estimated when χ'_{cc} is assumed to show a peak at $\omega\tau=1$, where $\omega(=2\pi f)$ is the angular frequency of AC magnetic field. We will show that the temperature (*T*) dependence of τ is well described in terms of a generalized Arrhenius law.

II. EXPERIMENTAL

Single crystals of natural vermiculite contain Mg^{2+} ions in the interlamellar space, forming Mg VIC. Samples used in the present work were prepared from natural vermiculites obtained from Llano, Texas. They were immersed in a 1 N aqueous solution of nickel chloride at 60 °C. Mg^{2+} ions can be replaced by Ni^{2+} ions, forming Ni VIC. The unit-cell stoichiometry of Ni VIC and Mg VIC with two-WL HS is given by $X\ Ni_u(H_2O)_{6.37}$ and $X\ Mg_{0.93}(H_2O)_{7.81}$, respectively, where $X=(Si_{5.72}Al_{2.28})(Mg_{5.88}Al_{0.10}Fe_{u'}Ti_{0.02})O_{20}(OH)_4$, $u'(=0.03)$ is the number of Fe ions in the octahedral sheet, and $u(=0.76\pm0.08)$ is the number of Ni^{2+} ions in the interlamellar space.[2] The total molar mass of the unit-cell stoichiometry for Ni VIC and Mg VIC is estimated as $M_{Ni}=917$ and $M_{Mg}=921$ g, respectively. The *c*-axis stacking structure of Ni VIC with two-WL HS was examined using (00L) x-ray diffraction. Figure 1 shows the (00L) x-ray diffraction pattern of Ni VIC with two-WL HS at 300 K. The Bragg peaks appear at the wave numbers given by $Q_c=(0.4385\pm0.0002\,\text{Å}^{-1})n$ with $n=1,2,\ldots,18$. The *c*-axis repeat distance *d* was determined as $d=14.330\pm0.007$ Å, which is close to that reported by Zhou *et al.* ($d=14.36\pm0.01$ Å).[4]

The DC magnetization and AC magnetic susceptibility of Ni VIC and Mg VIC were measured using a SQUID magnetometer (Quantum Design, MPMS XL-5) with an ultralow-field capability option.

(i) SQUID DC *magnetization.* Before setting up a sample at 298 K, a remanent magnetic field in the superconducting magnet was reduced to less than 3 mOe using an ultralow-field capability option. For convenience, hereafter this remanent field is noted as the state $H=0$. The sample was cooled from 298 to 1.9 K at $H=0$. After an external magnetic field ($H=1$ Oe) was applied at 1.9 K, the zero-field cooled magnetization (M_{ZFC}) was measured with increasing *T* from 1.9 to 50 K. The sample was heated up to 80 K and annealed at 80 K for 20 mins. Subsequently the field-cooled magnetization (M_{FC}) was measured with decreasing *T* from 50 to 1.9 K in presence of the same *H*. The DC magnetic susceptibility was also measured between 2 and 298 K in the presence of $H(=10\,\mathrm{kOe})$.

(ii) SQUID AC magnetic susceptibility ($\chi=\chi'+i\chi''$). A sample was cooled from 298 to 1.9 K at $H=0$. Then both χ' and χ'' were simultaneously measured with increasing *T* from 1.9 to 30 K in the absence of *H*, where the frequency and amplitude of the AC magnetic field were $f=0.07$ Hz -1 kHz and $h=1-2$ Oe, respectively. The measurement ($f=1$ and 10 Hz) was also carried out in the presence of various *H* with increasing *T* from 1.9 to 30 K, where *H* was changed at 1.9 K before each measurement.

The magnetic field was applied to either the *c* axis or any direction perpendicular to the *c* axis. For convenience, hereafter we use the word "*a* axis" for any direction in the *c* plane since there may be no magnetic anisotropy in the *c* plane.

III. RESULT

A. Magnetic susceptibility for Ni VIC and Mg VIC

Figure 2 shows the *T* dependence of DC magnetic susceptibility for Ni VIC with two-WL HS in the presence of $H(=10\,\mathrm{kOe})$ along the *c* axis and *a* axis. The magnetic susceptibility decreases with increasing *T*, obeying the Curie-Weiss law. The susceptibility along the *c* axis (χ_c) is larger than that along the *a* axis (χ_a). The least squares fit of the data for $50\leqslant T\leqslant 298$ K to the Curie-Weiss form

$$\chi_g=\chi_g^0+\frac{C_g}{T-\Theta}, \tag{1}$$

yields the parameters $\chi_g^0=(6.943\pm0.068)\times10^{-7}$ emu/g, $C_g=(1.330\pm0.001)\times10^{-3}$ emu K/g, and $\Theta=12.33\pm0.04$ K for the *c* axis, and $\chi_g^0=(-10.737\pm0.066)\times10^{-7}$ emu/g, $C_g=(1.267\pm0.001)\times10^{-3}$ emu K/g, and $\Theta=6.13\pm0.05$ K for the *a* axis.

We have also measured the DC magnetic susceptibility of the parent Mg VIC with two-WL HS, obeying the Curie-

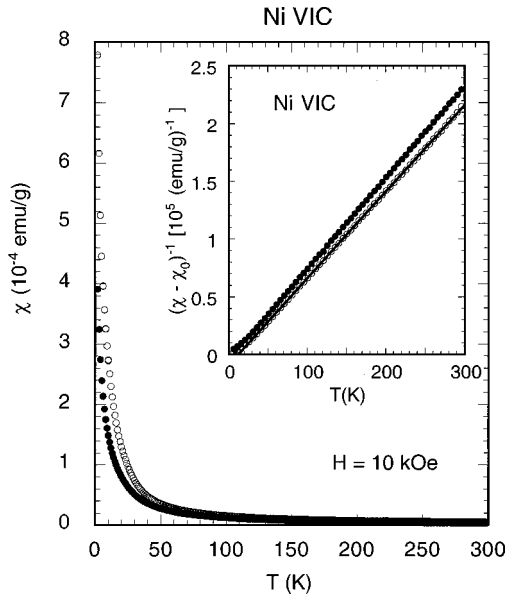

FIG. 2. T dependence of DC magnetic susceptibility χ_c (○) and χ_a (●) for Ni VIC. $H=10$ kOe. The inset shows the reciprocal susceptibility $(\chi-\chi_0)^{-1}$ as a function of T for Ni VIC. The solid lines denote the least-squares fits of the data to Eq. (1) with parameters given in the text.

Weiss law. The corresponding parameters are given by $\chi_g^0=(-6.223\pm0.044)\times10^{-7}$ emu/g, $C_g=(1.278\pm0.011)\times10^{-4}$ emu K/g, and $\Theta=-1.16\pm0.43$ K for the c axis, and $\chi_g^0=(-5.258\pm0.057)\times10^{-7}$ emu/g, $C_g=(1.305\pm0.013)\times10^{-4}$ emu K/g, and $\Theta=-0.99\pm0.49$ K for the a axis. Since Mg^{2+} ion has no magnetic moment, the Curie-Weiss susceptibility of Mg VIC with two-WL HS arises from impurity Fe^{2+} or Fe^{3+} ions, which exist in the octahedral sheet. The gram Curie-Weiss constant C_g of Mg VIC can be described by

$$C_g=u' P_{\mathrm{eff}}^2(\mathrm{Fe})/8M_{\mathrm{Mg}}, \tag{2}$$

with $u'=0.03$. The effective magnetic moment of Fe ion can be estimated as P_{eff} (Fe) $=5.602\pm0.024\,\mu_B$ for $H\|c$ and $5.661\pm0.028\,\mu_B$ for $H\|a$, which is between typical values of P_{eff} for $Fe^{2+}(\approx5.4\,\mu_B)$ and for $Fe^{3+}(\approx5.9\,\mu_B)$.[7] The gram Curie-Weiss constant C_g for Ni VIC can be described by[2]

$$C_g=\frac{1}{8M_{Ni}}[uP_{\mathrm{eff}}^2(\mathrm{Ni}^{2+})+u' P_{\mathrm{eff}}^2(\mathrm{Fe})], \tag{3}$$

where $P_{\mathrm{eff}}(\mathrm{Ni}^{2+})$ and $P_{\mathrm{eff}}(\mathrm{Fe})$ are the effective magnetic moments of Ni^{2+} in the interlamellar space and the Fe ion in the octahedral sheet. The effective magnetic moment $P_{\mathrm{eff}}(\mathrm{Ni}^{2+})$ can be estimated as $3.406\pm0.003\mu_B$ for $H\|c$ and $3.311\pm0.002\mu_B$ for $H\|a$, which are slightly larger than a typical value of P_{eff} for $Ni^{2+}(\approx3.2\mu_B)$.[7] The positive value of Θ in Ni VIC indicates that the nearest-neighbor exchange interaction between Ni^{2+} spins is ferromagnetic.

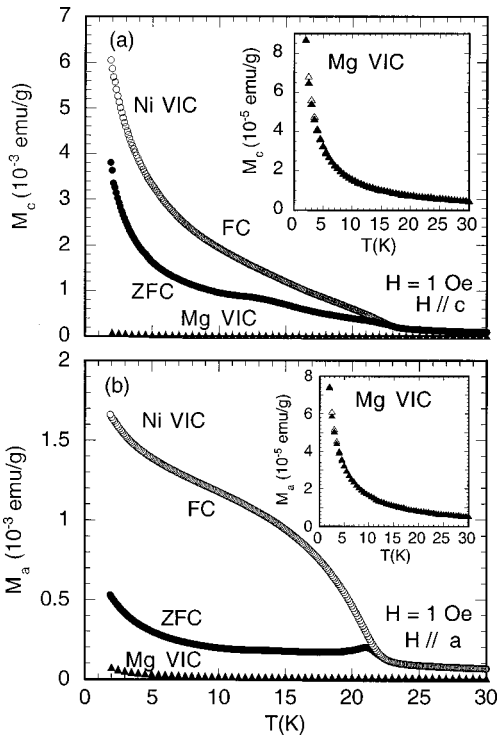

FIG. 3. T dependence of M_{FC} (○) and M_{ZFC} (●) for Ni VIC. $H=1$ Oe. (a) $H\|c$. (b) $H\|a$. The corresponding data of M_{FC} (△) and M_{ZFC} (▲) for Mg VIC with two-WL HS are also shown in the insets. $H=1$ Oe. (a) $H\|c$. (b) $H\|a$.

B. M_{FC} and M_{ZFC} along the c axis and a axis

Figure 3(a) shows the T dependence of M_{FC} and M_{ZFC} for Ni VIC in the presence of $H(=1$ Oe) along the c axis. Both M_{FC} and M_{ZFC} start to increase with decreasing T below 23.4 K. M_{FC} becomes larger than M_{ZFC} below 23.0 K, showing an irreversible effect of magnetization. In the inset of Fig. 3(a) for comparison we show the T dependence of M_{FC} and M_{ZFC} for Mg VIC in the presence of $H(=1$ Oe) along the c axis. Both M_{FC} and M_{ZFC} decrease with increasing T. There is no appreciable irreversible effect of magnetization. The magnitudes of M_{FC} and M_{ZFC} are much smaller than those of Ni VIC. Figure 3(b) shows the T dependence of M_{FC} and M_{ZFC} for Ni VIC in the presence of $H(=1$ Oe) along the a axis, which is rather different from that along the c axis. M_{ZFC} has a peak at 21.0 K, while M_{FC} drastically increases with decreasing T below 23 K. For convenience we define a Néel temperature T_N as the peak temperature of M_{ZFC}: $T_N=21.0$ K. In the inset of Fig. 3(b), for comparison we show the T dependence of M_{FC} and M_{ZFC} for Mg VIC ($H\|a$).

C. χ'_{cc} and χ''_{cc} at $H=0$

Figures 4(a) and 5(a) show the T dependence of χ'_{cc} for Ni VIC with various f. The dispersion χ'_{cc} has a sharp peak below 3.3 K. The peak shifts to the low-T side with decreasing f: 2.0 K at $f=0.07$ Hz and 3.30 K at $f=1$ kHz [see Fig. 5(a)]. The f dependence of the peak temperature will be discussed in Sec. IV C. There are two anomalous behaviors at high T: shoulders around 22.2 and 13.8 K [see the inset of

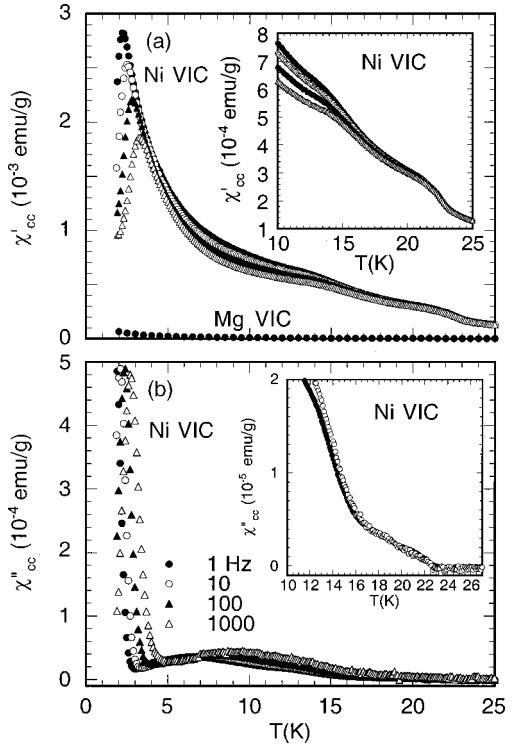

FIG. 4. T dependence of (a) χ'_{cc} and (b) χ''_{cc} for Ni VIC at various f: $f=1$ (●), 10 (○), 100 (▲), and 1000 Hz (△). $h=2$ Oe. $H=0$. The corresponding data of χ'_{cc} for Mg VIC are also shown in (a): $f=1$ Hz (●).

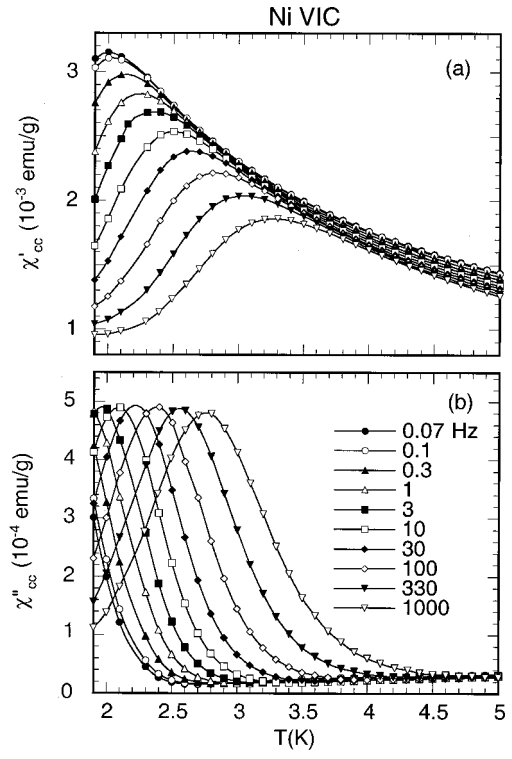

FIG. 5. T dependence of (a) χ'_{cc} and (b) χ''_{cc} for Ni VIC at various f ($0.07 \leqslant f \leqslant 1000$ Hz). $h=2$ Oe. $h \| c$. $H=0$. The solid lines are guides to the eye.

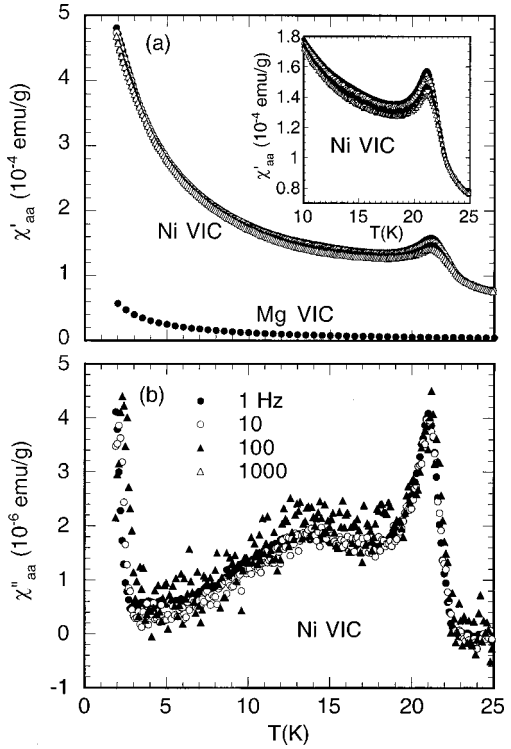

FIG. 6. T dependence of (a) χ'_{aa} and (b) χ''_{aa} for Ni VIC at various f: $f=1$ (●), 10 (○), 100 (▲), and 1000 Hz (△). $h=2$ Oe. $h \| a$. $H=0$. In (a) the corresponding data of χ'_{aa} for Mg VIC are also shown: $f=1$ Hz (●).

Fig. 4(a)]. In Fig. 4(a), for comparison we show the T dependence of χ'_{cc} for Mg VIC at $f=1$ Hz.

Figures 4(b) and 5(b) show the T dependence of χ''_{cc} for Ni VIC with various f. The absorption χ''_{cc} has a sharp peak at low T. It shifts to the low-T side with decreasing f:2.0 K at 3 Hz and 2.75 K at 1 kHz [see Fig. 5(b) for the detail]. The absorption χ''_{cc} exhibits a broad peak at higher T. The peak shifts to the low-T side with decreasing f (6.08 K at 0.07 Hz and 9.1 K at 1 kHz). Note that χ''_{cc} also shows a kink around 16.2 K and reduces to zero around 23.0 K [see the inset of Fig. 4(b)].

D. χ'_{aa} and χ''_{aa} for $H=0$

Figure 6(a) shows the T dependence of χ'_{aa} for Ni VIC with various f. The dispersion χ'_{aa} shows a peak at 21.1 K. This peak temperature is independent of f for $1 \leqslant f \leqslant 1000$ Hz, while the magnitude of the peak increases with decreasing f. In contrast to χ'_{cc}, below 21.1 K, χ'_{aa} increases with decreasing T and does not show any anomaly. For comparison we also show the T dependence of χ'_{aa} for Mg VIC at $f=1$ Hz. The value of χ'_{aa} is much smaller than that for Ni VIC. Figure 6(b) shows the T dependence of χ''_{aa} for Ni VIC with various f. The absorption χ''_{aa} has a sharp peak at 21.0 K for $f=1$ and 10 Hz and at 21.2 K for $f=100$ and 1000 Hz. The absorption χ''_{aa} also has a broad peak at 13.6 K for $f=1$ Hz and 14.4 K for $f=10$ Hz, and a sharp peak that shifts to the low T side with decreasing f (2.08 K at $f=1$ Hz and 2.8 K at 1 kHz).

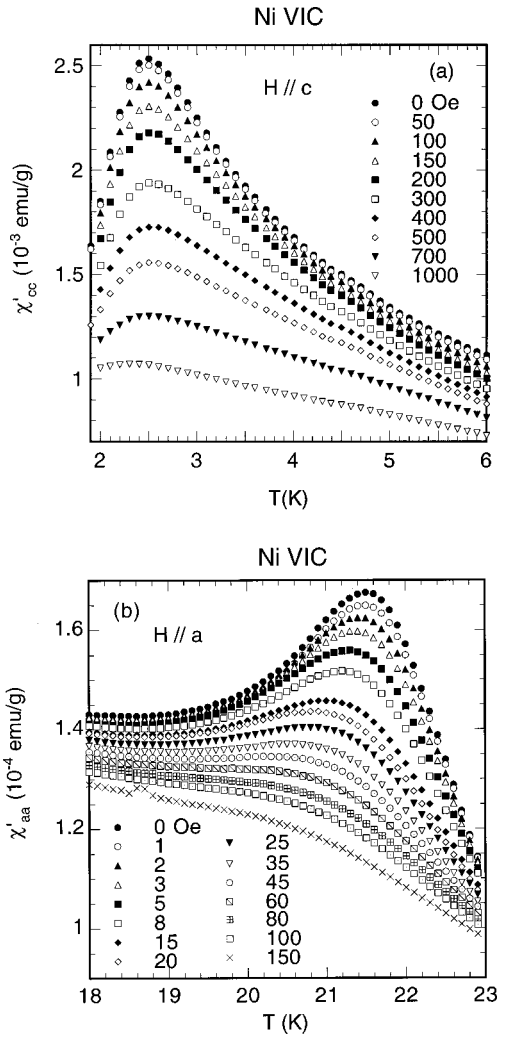

FIG. 7. (a) T dependence of χ'_{cc} for Ni VIC at various H. $H\|h\|c$. $f=10$ Hz. $h=2$ Oe. (b) T dependence of χ'_{aa} for Ni VIC at various H. $H\|h\|a$. $f=1$ Hz. $h=2$ Oe.

E. χ'_{cc}, χ''_{cc}, χ'_{aa}, and χ''_{aa} at $H\neq 0$

Figure 7(a) shows the T dependence of χ'_{cc} at various H along the c axis, where $f=10$ Hz and $h=2$ Oe. The dispersion χ'_{cc} shows a peak at 2.5 K for $H=0$, which does not shift with H at least up to 700 Oe. Similar behavior is observed in χ''_{cc}: the peak at 2.1 K for $H=0$ does not shift with H at least up to 500 Oe. These results suggest that the peak around 2–3 K may have nothing to do with a possible spin order in Ni^{2+}. Figure 7(b) shows the T dependence of χ'_{aa} at various H along the a axis, where $f=1$ Hz and $h=2$ Oe. The peak shifts to the low-T side with increasing H, suggesting the antiferromagnetic nature of phase transition at T_N.

IV. DISCUSSION

A. Short-range spin order above T_N

We discuss a possibility of short-range spin order in the paramagnetic phase above T_N. Figure 8 shows the T dependence of the difference between $M_{\rm FC}$ along the c axis and $M_{\rm FC}$ along the a axis for Ni VIC, defined by $\Delta M_{\rm FC}=M^c_{\rm FC}-M^a_{\rm FC}$, where $H=1$ Oe. The difference $\Delta M_{\rm FC}$ is positive for any T, showing that the spin easy direction is the c axis. It decreases with increasing T, except for the local maximum near $T_N(=21.0\,{\rm K})$ (see the inset of Fig. 8). Figure 9 shows the T dependence of the difference between χ_c and χ_a for Ni VIC, defined by $\Delta\chi=\chi_c-\chi_a$, where $H=10$ kOe. The difference $\Delta\chi$, which is positive for any T, decreases with increasing T. Unlike $\Delta M_{\rm FC}$, there is no anomaly in $\Delta\chi$ around T_N. Nagata *et al.*[8] have predicted the following equation for a system with an uniaxial spin symmetry referred to the c axis

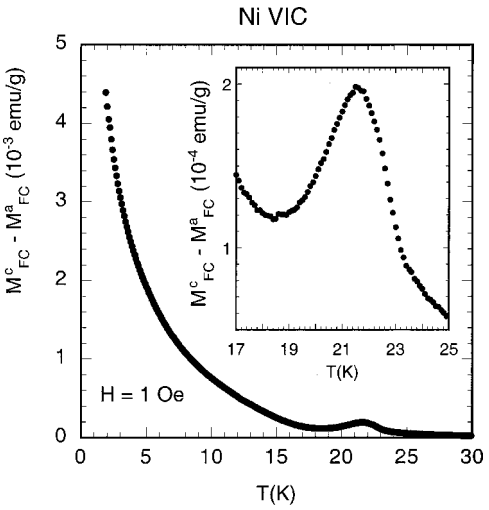

FIG. 8. T dependence of $\Delta M_{\rm FC}(=M^c_{\rm FC}-M^a_{\rm FC})$ at $H=1$ Oe for Ni VIC. The detail near T_N is shown in the inset.

$$\left(\frac{k_BT}{\mu_B}\right)^2\left[\frac{\chi_c}{g_c^2}-\frac{\chi_a}{g_a^2}\right]=\sum_{j,l}\sum_{k,m}(K^{cc}_{jl}-K^{aa}_{jl})\times\langle S^c_jS^c_l(S^c_kS^c_m-S^a_kS^a_m)\rangle, \qquad (4)$$

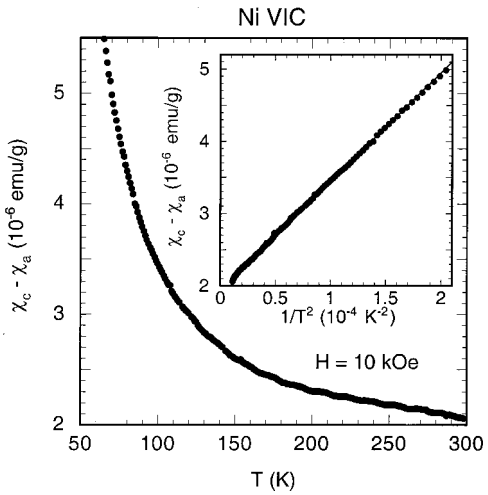

FIG. 9. T dependence of $\Delta\chi(=\chi_c-\chi_a)$ at $H=10$ kOe for Ni VIC. The inset shows the plot of $\Delta\chi$ as a function of T^{-2}. The solid line denotes the least-squares fit of the data to Eq. (5) with parameters given in the text.

where K_{jl} represents the anisotropic exchange interaction and magnetic dipole-dipole interaction between spins S_j and S_l, and $\langle\cdots\rangle$ refers to a thermal average in $H=0$. If the short-range order effect is negligible in the paramagnetic phase, the difference $\Delta\chi$ must be proportional to T^{-2} because of the isotropic g factor. In the inset of Fig. 9, we show $\Delta\chi$ for Ni VIC as a function of T^{-2}. The difference $\Delta\chi$ is well described by

$$\chi_c-\chi_a=a_1+a_2/T^2, \tag{5}$$

with $a_1=(1.937\pm0.002)\times10^{-6}$ emu/g and $a_2=(1.507\pm0.002)\times10^{-2}$ emu K^2/g for $70\leqslant T\leqslant298$ K. The deviation of $\Delta\chi$ from Eq. (5) is clearly observed below 45 K, suggesting the 2D short-range order persists up to $\approx2T_N$.

The T dependence of $\Delta\chi$ for Mg VIC is rather different from that for Ni VIC. The sign of $\Delta\chi$ changes from positive to negative at 5.7 K as T increases. It exhibits a negative local minimum around 10–11 K, increasing with further increasing T. The susceptibility $\Delta\chi$ for Mg VIC is also well described by Eq. (5) with $a_1=(-1.047\pm0.003)\times10^{-7}$ emu/g and $a_2=(-1.632\pm0.011)\times10^{-4}$ emu K^2/g for $70\leqslant T\leqslant298$ K. These results suggest that the spin easy direction is in the c plane for Fe ions in the octahedral sheet in Mg VIC at high T. The spin symmetry of Fe ions changes from XY-like to Ising-like below 5.7 K. The dipole-dipole interaction between Ising Ni^{2+} spins and Ising Fe spins may favor a ferromagnetic spin alignment for them in Ni VIC.

B. Nature of antiferromagnetic phase transition at T_N

We determine the value of u for Ni VIC from the value of the saturation magnetization M_s: $M_s=16$ emu/g along the c axis for Ni VIC with two-WL H5,[3] The saturation magnetization M_s (emu/g) in Ni VIC is described by

$$M_s\ \text{(emu/g)} = 5584.9[ug_c(\text{Ni})S(\text{Ni})+u'g_c(\text{Fe})S(\text{Fe})]/M_{\text{Nl}}, \tag{6}$$

where $g_c(i)$ and $S(i)$ are the g factor along the c axis and spin for $i=$Ni and Fe, $g_c(\text{Ni})=2.38$,[9] $u'=0.03$, and $M_{\text{Ni}}=917$. The value of u can be estimated as $u=1.04$ for Fe^{3+} with $S(Fe^{3+})=\frac{5}{2}$ and $g_c(Fe^{3+})\approx2$, and as $u=1.05$ for the case of Fe^{2+} with $S(Fe^{2+})=2$ and $g_c(Fe^{2+})\approx2$. These values of u are relatively larger than our result obtained in the previous work ($u=0.76$).[2]

In the previous work[2] we have discussed the in-plane structure of magnetic VIC's in light of a mixed phase formed of possible commensurate structures with $u=2$, $\frac{4}{3}$, 1, and $\frac{2}{3}$, where u is the number of magnetic ions per a rectangular unit cell of $(a\times b)$ with $a=5.34$ Å and $b=9.30$ Å. We have claimed that the in-plane structure of Ni^{2+} in VIC is formed of the combination of commensurate structures with $u=1$ and $\frac{2}{3}$ type of in-plane structures at the ratio of 0.28:0.72. This model may not be appropriate for the explanation of the intraplanar exchange interaction observed in Ni VIC: the distance between N^{2+} ions may be too large for the superexchange interaction mechanisms. What is a suitable in-plane structure model for Ni VIC? Figure 10 shows the in-plane structure model of magnetic VIC's with $u=2$. The magnetic ions may sit over m_1 or m_2. The m_1 and m_2 sites are located between those triangular groups of surface oxygens forming the bases of the SiO_2 and AlO_4 tetrahedrons. The magnetic ions for $u=2$ form an isosceles triangular lattice with one side $a=5.34$ Å and two sides $a'=(a^2+b^2)^{1/2}=5.36$ Å. Since the value of $u(=0.76)$ for Ni VIC is smaller than that in Mg VIC ($u=0.93$), there is a possibility that a part of Mg^{2+} ions may not be replaced by Ni^{2+} ions, probably due to slow diffusion. We also note that from a viewpoint of magnetic properties, vacant sites are equivalent to sites occupied by nonmagnetic Mg^{2+} ions. For the Ni concentration $c=u/2<1$, a part of Ni^{2+} ions are randomly replaced by vacant sites or Mg^{2+} ions, forming a diluted site-random Ising ferromagnetic system.

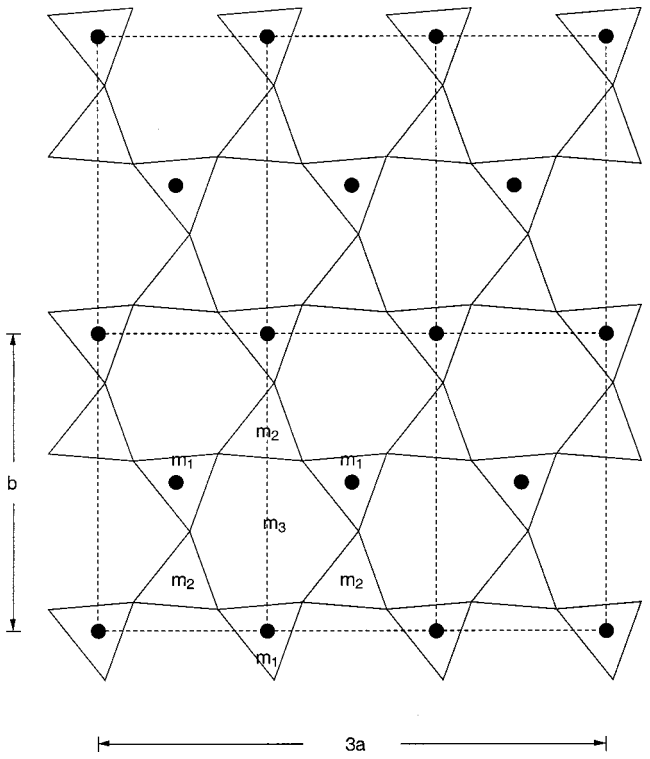

FIG. 10. Commensurate in-plane structure model for Ni VIC with $u=2$. $a=5.34$ Å and $b=9.30$ Å. See Ref. 2 for the detail of structure.

Since the ferromagnetic intraplanar exchange interaction J is dominant over the antiferromagnetic interplanar exchange interactions J', Ni VIC is regarded as a 2D site-random ferromagnetic system on the triangular lattice site. The percolation threshold c_p is predicted to be 0.5.[10] Below c_p there is no long-range spin order at any finite T. For $u=0.76$, the Ni concentration $c(=u/2=0.38)$ is lower than $c_p^{2D}(=0.5)$, suggesting no occurrence of long-range spin order in each Ni layer. For $u=1.05$ obtained from the saturation magnetization measurement, the Ni concentration ($c=u/2=0.525$) is a little higher than c_p^{2D}, suggesting the possibility of long-range spin order.

How can we explain the antiferromagnetic phase transition at T_N in Ni VIC? First we consider an ideal case (c

$=u/2=1$), where all the triangular lattice sites in the Ni layer are occupied by Ni ions. The nature of magnetic phase transition may be very similar to that of $Ni(OH)_2$.[11] Note that $Ni(OH)_2$ undergoes a 3D Ising antiferromagnet ($T_N = 26.4\,K$). On approaching T_N from the high T side, the ferromagnetic short-range order grows in each Ni layer. The effective antiferromagnetic interplanar interaction defined by $J'_{eff}=J'(\xi_{in}/a)^2$ divergingly increases as the in-plane spin correlation length ξ_{in} increases, where a is the in-plane lattice constant. Below T_N where the magnitude of J'_{eff} is larger than that of J, the 2D ferromagnetic long-range order is established in each Ni^{2+} layer. Such 2D ferromagnetic layers are antiferromagnetically coupled along the c axis, forming an antiferromagnetic order.

According to the percolation theory,[10] the Néel temperature T_N decreases with decreasing Ni concentration and reduces to zero below c_p. Since the Ni concentration of Ni VIC is $c=u/2=0.38$ or 0.525, T_N is predicted be close to 0 K, which is inconsistent with our result that Ni VIC undergoes the antiferromagnetic phase transition at $T_N(=21.0\,K)$. This suggests that Ni^{2+} ions may not be randomly distributed on the lattice sites. One possibility is that Ni ions may be formed of small islands inside the Ni layers. The Ni ions in each island are uniformly located on the triangular lattice sites. Similar behavior is observed in stage-2 $CoCl_2$ graphite intercalation compound.[12] The diameter of islands L may be large enough such that $J\approx|J'|(L/a)^2$. There is no structural and magnetic correlation between islands. Below T_N, Ni spins are ferromagnetically ordered inside islands. These ferromagnetic islands are antiferromagnetically coupled with islands in the other layers, forming antiferromagnetic clusters. Because the growth of the in-plane correlation length is suppressed by the size L, the resultant antiferromagnetic clusters do not show any true 3D long-range order.

C. Superparamagnetic behavior around 2–3 K

As shown in Figs. 5(a) and 5(b) the peaks of χ'_{cc} and χ''_{cc} around 2–3 K shift to the low-T side with decreasing f. Does this anomaly suggest an occurrence of reentrant spin-glass (RSG) phase transition as phenomenon as a thermally equilibrium state or a manifestation of a superparamagnetic behavior as a thermally nonequilibrium state? The T dependence of the average relaxation time τ provides a key to determining which mechanism is appropriate. The relaxation time can be estimated under an assumption that the peaks of χ'_{cc} and χ''_{cc} occur when $\omega\tau=1$, where $\omega(=2\pi f)$ is the angular frequency of the AC field. Figure 11 shows τ as a function of T, which is obtained from the data of χ'_{cc} vs T and χ''_{cc} vs T with various f, respectively. The relaxation times divergingly increase with decreasing T. Here we note that τ derived from χ'_{cc} is much longer than that from χ''_{cc} for the same T. This discrepancy may be partly due to our assumption that the peak of χ'_{cc} occurs when $\omega\tau=1$. In a simple Debye-type relaxation with a single-relaxation time, χ'_{cc} shows no peak at any $\omega\tau$, while χ''_{cc} shows a peak at $\omega\tau=1$.

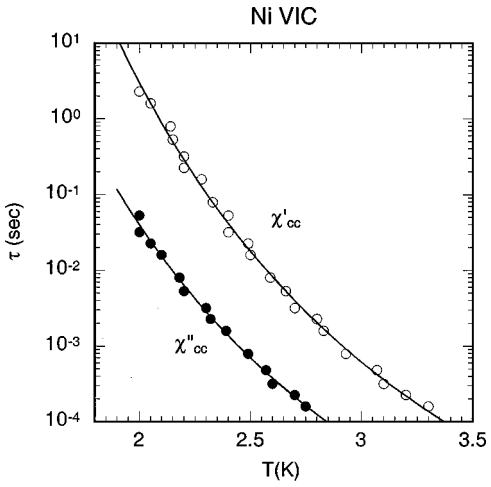

FIG. 11. T dependence of τ that is determined from the f dependence of peak temperature in the data of χ'_{cc} vs T [Fig. 5(a)] (○) and χ''_{cc} vs T [Fig. 5(b)] (●). The solid lines denote the least-squares fits of the data to a generalized Arrhenius law given by Eq. (7). The parameters are given in the text.

The most likely source of such a dramatic divergence of τ is a thermally activated relaxation over energy barriers. The basic idea of activated dynamics is to define a droplet in the ground state as the lowest-energy excitation of length scale L.[13] The thermal activation over energy barrier height $B(\approx L^{\psi})$ is assumed for the droplets that are thermally active, where ψ is an exponent. The relaxation time for the droplet with $L(=\xi)$ is given by a generalized Arrhenius law

$$\tau=\tau_0\exp\left(\frac{B}{T}\right),$$

or

$$\ln\left(\frac{\tau}{\tau_0}\right)=\left(\frac{b}{T}\right)^{1+\psi\nu}, \tag{7}$$

where ξ is the spin correlation length, $\xi\approx T^{-\nu}$ for a zero-temperature critical point, ν is a critical exponent of ξ, τ_0 is the microscopic single-spin relaxation time, and $B=b^{1+\psi\nu}/T^{\psi\nu}$. A simple Arrhenius law corresponds to the case of $\psi\nu=0$. As far as we know, no theoretical value of $\psi\nu$ has been reported. The least-squares fits of the data τ vs T as shown in Fig. 11 to Eq. (7) yield $\tau_0=(1.5\pm0.4)\times10^{-10}$ sec, $1+\psi\nu=1.09\pm0.20$, and $b=36.5\pm1.1$ K for $2\leqslant T\leqslant3.3$ K in χ'_{cc}, and $\tau_0=(1.0\pm0.5)\times10^{-10}$ sec, $1+\psi\nu=1.02\pm0.49$, and $b=37.0\pm0.8$ K for $2\leqslant T\leqslant2.75$ K in χ''_{cc}. The least-squares fitting curves thus obtained, are denoted by solid lines in Fig. 11. The values of $\psi\nu$ are close to zero corresponding to the Arrhenius law. The barrier height $B(=b^{1+\psi\nu}/T^{\psi\nu})$ is weakly dependent on T and is roughly estimated as 47 K and 39 K for χ'_{cc} and χ''_{cc}, respectively, at $T=2$ K near the peak temperatures of χ'_{cc} and χ''_{cc}.

When the Arrhenius law ($\psi\nu=0$) is assumed, b is equal to the activation energy $E_a(=B)$ separating the states. For typical systems governed by the Arrhenius law, τ_0 is considered to be on the order of 10^{-9} sec.[14] The blocking tempera-

ture T_B is considered to be on the order of $E_a/25k_B$.[14] Below T_B, the relaxation time becomes long enough to be observable on a laboratory time scale. Our result indicates that τ_0 is on the order of 10^{-10} sec and that $E_a \approx b = 37$ K. The blocking temperature T_B is estimated as 1.5 K using the relation $T_B \approx E_a/25k_B$, which is close to the peak temperatures of χ'_{cc} and χ''_{cc}. It is experimentally known that the frequency shift of the peak temperature T_p of χ' defined by μ $(=\Delta T_p/T_p$ per decade $\omega)$ also provides a criterion for distinguishing between superparamagnet and spin glass.[14] The value of μ for superparamagnet is much larger than that for canonical spin glasses: $\mu = 0.28$ for amorphous $(Ho_2O_3)(B_2O_3)$ as a superparamagnet and $\mu = 0.005$ for CuMn as a canonical spin glass. In our system the value of μ is roughly estimated as 0.24 for a decade ω of $100 \leqslant f \leqslant 1000$ Hz, 0.17 for $10 \leqslant f \leqslant 100$ Hz, and 0.11 for $1 \leqslant f \leqslant 10$ Hz, where T_p is assumed to be 2 K. Such a high ratio μ supports that Ni VIC shows a superparamagnetic behavior around 2–3 K. Thus it can be concluded from these results that the peaks of χ'_{cc} and χ''_{cc} around 2–3 K can be explained in terms of the generalized Arrhenius law with $\psi\nu \sim 0$. The system may be a superparamagnet consisting of small magnetic clusters. Spins inside each cluster are antiferromagnetically ordered. There is no interaction between magnetic clusters. No long-range-ordered phase exists.

We also discuss whether the T dependence of τ for χ'_{cc} can be described in terms of a power-law form

$$\tau = \tau_0^*(T/T^* - 1)^{-x}, \tag{8}$$

where $x = z\nu^*$, z is the dynamic critical exponent, ν^* is the exponent of the spin correlation length, T^* is a finite critical temperature, and τ_0^* is a characteristic time. The least-squares fit of the data of τ vs T over the temperature range of 1.9–3.3 K to Eq. (8) yields the parameters $x = 8.65 \pm 0.85$, $T^* = 1.42 \pm 0.10$ K, and $\tau_0^* = (1.53 \pm 0.30) \times 10^{-3}$ sec. The value of τ_0^* is extremely longer than that ($\tau_0^* = 1.58 \times 10^{-13}$ sec) for a typical 3D Ising spin glass $Fe_{0.5}Mn_{0.5}TiO_3$,[15] suggesting that the model of critical slowing down is not appropriate for the present system.

As shown in Fig. 4(b), we observe a broad peak in χ''_{cc} around 6–9 K, which shifts to the high-T side with increasing f. As shown in Fig. 6(b) we also observe a broad peak in χ''_{aa} around 13.6–14.4 K which slightly shifts to the high-T side with increasing f. These anomalies may be related to the disordered nature of antiferromagnetic phase below T_N. However, the origin is not fully understood at present.

V. CONCLUSION

Ni VIC with two-WL HS magnetically behaves like a diluted site-random spin system with Ising symmetry along the c axis. This compound undergoes a partially disordered antiferromagnetic phase transition at T_N. A superparamagnetic behavior around 2–3 K suggests that the system consists of small magnetic clusters antiferromagnetically ordered. Magnetic neutron-scattering studies on Ni VIC where all hydrogen atoms are replaced by deuterium, would be required for further understanding the nature of antiferromagnetic clusters.

ACKNOWLEDGMENTS

We would like to thank K. Koga and H. Nishihara for their useful discussions at the early stage of the present work. The work at SUNY Binghamton was partially supported by NSF DMR 8902351 and 981098.

*Email address: suzuki@binghamton.edu

[1] N. Wada, M. Suzuki, D. R. Hines, K. Koga, and H. Nishihara, J. Mater. Sci. **2**, 864 (1987).
[2] M. Suzuki, M. Yeh, C. R. Burr, M. S. Whittingham, K. Koga, and H. Nishihara, Phys. Rev. B **40**, 11 229 (1989), and references therein.
[3] H. Nishihara, G. Kido, K. Koga, M. Suzuki, N. Wada, and Y. Nakamura, J. Magn. Magn. Mater. **90 & 91**, 81 (1990).
[4] P. Zhou, J. Amarasekera, S. A. Solin, S. D. Mahanti, and T. J. Pinnavaia, Phys. Rev. B **47**, 16 486 (1993).
[5] I. S. Suzuki, J. Morrilo, C. R. Burr, and M. Suzuki, Phys. Rev. B **50**, 205 (1994).
[6] M. Suzuki, N. Wada, D. R. Hines, and M. S. Whittingham, Phys. Rev. B **36**, 2844 (1987), and references therein.
[7] See, for example, C. Kittel, *Introduction to Solid State Physics*, 7th ed. (Wiley, New York, 1996).
[8] K. Nagata, I. Yamamoto, H. Takano, and Y. Yokozawa, J. Phys. Soc. Jpn. **43**, 857 (1977).
[9] K. Koga and H. Nishihara (unpublished).
[10] R. B. Stinchcombe, in *Phase Transitions and Critical Phenomena*, edited by C. Domb and J. L. Lebowitz (Academic, London, 1983), Vol. 7, p. 151.
[11] M. Suzuki, I. S. Suzuki, and T. Enoki, J. Phys.: Condens. Matter **12**, 1377 (2000).
[12] M. Suzuki and I. S. Suzuki, Phys. Rev. B **58**, 840 (1998).
[13] D. S. Fisher and D. A. Huse, Phys. Rev. B **36**, 8937 (1987).
[14] J. A. Mydosh, *Spin Glasses: An experimental introduction* (Taylor and Francis, London, 1993).
[15] K. Gunnarsson, P. Svedlindh, P. Nordblad, L. Lundgren, H. Aruga, and A. Ito, Phys. Rev. Lett. **61**, 754 (1988).